ELSEVIER

Catalysis Today 41 (1998) 21–35

CATALYSIS TODAY

The chemistry of oxidation catalysts based on mixed oxides

F. Trifirò

Dipartimento di Chimica Industriale e dei Materiali, Viale Risorgimento 4, 40136 Bologna, Italy

Abstract

The chemistry of preparation of molybdates, of TiO_2 supported vanadium oxides and of V–P mixed oxides has been examined and discussed. The main factors which determine the nature of the active species are: (a) in the case of preparation of molydbates, the nature of molybdenum species in solution and the solid state reaction which free oxides; (b) in the case of preparation of supported vanadium oxide, the wetting by vanadium species of the support surface during the calcination and the reduction occurring at the vanadium sites during the reaction; and (c) in the case of preparation of V–P mixed oxide, the defective nature of the precursor and its transformation which occurs during the activation stage and under reaction conditions.

Keywords: Mixed oxides; Molybdenum; Vanadium

1. Introduction

The aim of this lecture is to report some examples of preparation of catalysts based on mixed oxides in order to evidence the different chemistry involved.

The main properties of the mixed oxides which are involved in the catalytic process are the following:

1. redox properties,
2. Lewis acidity,
3. Brønsted acidity,
4. basic properties,
5. surface coordination (unsaturative coordination of transition elements),
6. surface topology: types of neighbours near the transition element,
7. lattice oxygen mobility, and
8. presence of defects which are able to activate molecular oxygen.

In order to discuss the key factors involved in the preparation of catalysts based on mixed oxides the following examples will be considered in detail:

- Molybdenum based mixed oxides as catalysts for the allylic oxidation of olefins and oxidation of methanol to formaldehyde [1].
- $(VO)_2P_2O_7$ catalysts for the selective oxidation of *n*-butane to maleic anhydride [2].
- V_2O_5 supported on TiO_2 catalysts for the selective oxidation of *o*-xylene to phthalic anhydride [3].

2. The chemistry of preparations of molybdates

Molybdenum-based catalysts are widely used in oxidation and ammoxidation reactions of olefins and alcohols. In addition to molybdenum, Fe, Bi, Co, Mn, Ce and Te are added alone or in mixture in the various formulations of industrial catalytic systems [4].

0920-5861/98/$32.00
PII S0920-5861(98)00035-2

Table 1
Preparation conditions for several pure molybdates and tungstates

$Bi_2(MoO_4)_3$	pH=1.5, T=20°C, high Mo concentration
Bi_2MoO_6	Solid state reaction between Bi_2O_3 and $Bi_2Mo_2O_9$ or bismuth adsorption on $Bi_2MO_2O_9$ folllowed by solid state reaction
$Bi_2Mo_2O_9$	pH=2.2, T=80°C
$Bi_2W_2O_9$	pH=2.2, T=80°C
$Bi_2(WO_4)_3$	Solid state reaction between Bi_2O_3 and WO_3
Bi_2WO_6	Solid state reaction or adsorption of bismuth on $Bi_2W_2O_9$ and solid state reaction
$MnMoO_6$	pH=5.5, T>80°C
$CoMoO_4$	pH=5.5, T>80°C
$Fe_2(MoO_4)_3$	pH m=1.8, T>80°C, long aging
Te_2MoO_7	Solid state reaction at 500°C
$Ce_2(MoO_4)_3$	pH=7, T=20°C, low Mo conentration, aging

The most modern systems are the multicomponent complex ones, whereas in earlier formulations two-component systems were common; nevertheless this work places particular emphasis on the preparation of pure molybdates since it is the basis for the preparation of this class of catalysts and probably pure molybdates are present in the new industrial formulations either as matrices or as components with specific functions. Table 1 reports some of the particular experimental conditions for the preparation of some molybdates of elements generally mentioned in patent formulation of oxidation catalysts [5–8]. These conditions vary according to the molybdate considered.

The chemical factors responsible for the particular choice of the preparation conditions which will be discussed are the following:

1. Polymeric species of molybdenum ions present in aqueous solution.
2. Adsorption properties of some amorphous molybdates.
3. Formation of molybdenum heteropolyanions.
4. Evolution of the precipitate – transformation amorphous-crystalline.
5. Solid state reaction with oxide impurities at high temperature during calcination.

2.1. Polymeric species of molybdenum ions

In aqueous solution several molybdenum species can be present in equilibrium conditions, the nature and the relative ratio of which depend on the pH, temperature, and concentration. In Table 2 the effects of these variables are summarized.

The type of molybdenum ions present in solution (and the solubility of the salts they can give rise to) were proposed to determine the type of precipitate formed and therefore its stoichiometry.

This calculation was used in order to explain the type of Bi–molybdate formed by precipitation [7]. In fact only two compounds are formed directly by precipitation: Bi–Molybdate 2/3 and Bi–Molybdate 1/1 attributed, respectively, to the presence of $Mo_3O_{10}^{2-}$ and $Mo_2O_7^{2-}$ ions in aqueous solution. Results are summarized in Table 3.

The formation of Bi–Molybdate 2/1 occurs with another mechanism that will be explained below. Where Bi–tungstates are concerned, only Bi–tungstate 1/1 forms directly by precipitation. This was explained assuming that among the different W ions present in solution, $W_2O_7^{2-}$ only is able to give rise to a precipitate.

In the case of Co, Mn and Ce–molybdates under the most favourable condition for the precipitation (see Table 1), MoO_4^{2-} ionic species are present in aqueous solution. A very high pH, however, leads to an excess of second metal present as hydroxide inside the precipitate. On the contrary, at lower temperature a precipitate with (Mo/Mn)>1 is obtained; when calcined at higher temperature it gives rise to $MnMoO_4$ and MoO_3.

Table 2
Evolution of soluble molybdenum species with the variation of pH, temperature, Mo concentration

	Mo species						
	cis-Mo_2^+	$HMo_2O_6^+$	$Mo_2O_7^{2-}$	$Mo_4O_{13}^{2-}$	$Mo_8O_{24}^{4-}$	$Mo_7O_{24}^{6-}$	MoO_4^{2-}
pH	From→1→to→6						
Temperature	From r.t.→to→100°C						
Mo conc.	→Decreasing→						

Table 3
Range of conditions under which Bi–molybdates are formed

	Bi/Mo atomic ratios				
	No precipitate	2/3+MoO_3	2/3+1/1	2/1+1/1+2/3	2/1+1/1
pH	From 1→to→2.2				
Temperature	From 20°C→to→80°C				
Mo conc.	→Decreasing→				

The precipitate can be either the manganese salt of a polymeric Mo species (Table 2) or a salt of a Mn heteropolyanion as discussed in Section 2.3.

In the case of Co at low temperature or at low pH no precipitate forms because of the probable formation of a soluble Co–heteropolymolybdate.

In the case of Ce at lower pH and higher Mo concentration, an amorphous precipitate with (Mo/Ce) ratio higher than 1 forms, while at 100°C, where MoO_4^{2-} are present, $NH_4Ce(MoO_4)_2\ H_2O$ forms [1].

2.2. Adsorption properties of some amorphous molybdates

It is known that molybdates and tungstates display high exchange properties towards other types of ions. We have observed that Bi–molybdate 1/1 and Bi–tungstate 1/1 freshly prepared can adsorb bismuth or bismutyl ions when introduced in aqueous solution containing a bismuth salt. These adsorbed Bi-species can react with the matrix at high temperature by solid state reaction (T>400°C) giving rise to the respective 2/1 compounds [7,8].

2.3. Formation of heteropolyanions

Molybdenum together with many other elements can easily form heteropolyanions. Trivalent metals can give $[Me^{III}O_6(MoO_3)_6]^{3-}$ ions in solution and the respective salts [11]. Actually at pH 2 a precipitate [1] with a ratio (Mo/Fe)=2.5–3 (which is close to the theoretical one [5]) is obtained: therefore, the formation of this type of heteropolyanion is responsible for the impossibility in preparing pure $Fe(MoO_4)_3$ by simple precipitation.

Moreover, in the case of $Bi_2(MoO_4)$ Keulks advances that the nature of the precipitate is due to heteropolymolybdate of Te with a high Mo/Te ratio $[TeO_6(MoO_3)_6]^{8-}$.

In the case of Mn–molybdate an alternative explanation to the one already given, for the formation of precipitates with high Mo content when working at low pH and temperature, is the assumption of the formation of Mn heteropolymolybdate.

This explanation is more clearly evident in the case of Ce(II) molybdate since a high coloured orange solution is obtained from which at temperature below 5°C a precipitate is formed with a definite composition $Ce_2O_3{\cdot}14MoO_3{\cdot}nH_2O$, while electrophoresis shows to be an anionic complex [9]. At temperatures between 22°C and 30°C an amorphous precipitate with no well defined composition forms.

2.4. Evolution of the precipitate

In the case of the Fe(III) molybdate we observed an evolution of the nature of the precipitate [10] during the aging. The Fe–molybdate obtained by the precipitation at pH=1.8 both at room temperature or higher temperature (100°C) is an amorphous compound with Mo/Fe 2.5–3.

However, if the solid is recovered in the mother liquor for a few hours at 100°C a crystalline compound with Mo/Fe=1.5 is obtained. On the basis of X-ray pattern and IR spectrum it was found to correspond to pure $Fe_2(MoO_4)_3$. In Fig. 1 transformation of the precipitate and the most important properties of the compound so obtained are reported.

In the same figure it is shown that the amorphous compound decomposes at temperatures higher than 350°C into $Fe_2(MoO_4)_3$ and MoO_3, as already observed by other authors.

In Fig. 1 the activity and selectivity data of the above compounds in the oxidation of methanol to formaldehyde are also reported. Both catalysts are active and selective, showing practically the same activity per unit of surface area, but the pure one (Mo/Fe=1.5) has a powder consistence while the other is a hard

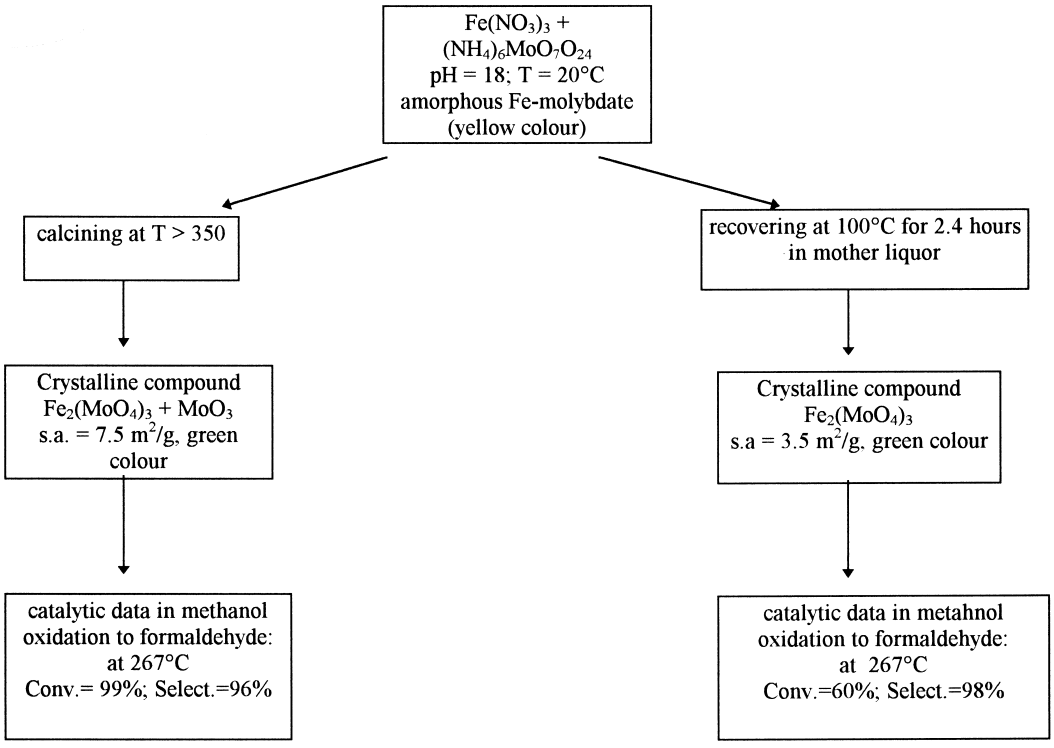

Fig. 1. Crystallization pathway of Fe/Mo/O species.

Table 4
Products obtained by solid state reactions between oxides and mixed oxides at 450°C in air

$Bi_2Mo_2O_9+Bi_2O_3 \rightarrow Bi_2MoO_6$
$Bi_2MoO_6+MoO_3 \rightarrow Bi_2(MoO_4)_3$
$Bi_2MoO_6+{}_2Bi_2O_3 \rightarrow Bi_6MoO_{12}$
$Bi_2(MoO_4)_3+Bi_2O_3 \rightarrow Bi_2MoO_6$
$Bi_2W_2O_9+Bi_2O_3 \rightarrow Bi_2WO_6$ (at 600°C)
$Fe_2(MoO_4)_3+Bi_2O_3 \rightarrow Bi_2(MoO_4)_3+Fe_2O_3$
$MnMoO_4+TeO_2 \rightarrow MnMoTeO_6$

solid. Further details about this can be found in [10].

2.5. *Solid state reactivity*

In Table 4 the solid state reactions that occur at 450°C are shown. The first point to be underlined in Table 4 is that in the case of Bi–molybdate and tungstates, new compounds can form during calcination or reaction operation due to the presence of an excess of one of the two oxides. Therefore, sometimes in working conditions the nature and the behaviour of the catalyst can differ from that introduced in the reactor. Besides, the occurrence of these solid state reactions can be utilized when the preparation is not practicable as it is in the case of Bi_6MoO_{12}, Bi_6WO_{12} and $Bi_2(WO_4)_3$.

3. The chemistry of preparation of V/P/O mixed oxides

Several industrial processes exist for the production of maleic anhydride from *n*-butane, which differ regarding the type of reactor and the method employed for maleic anhydride recovery and purification [2]. All processes employ the same kind of catalyst, based on a vanadium/phosphorus mixed oxide [11].

Different methods of preparation for the V/P/O catalysts have been reported, all of which achieve the ultimate active phase via the following stages:

1. Initial preparation of the active phase precursor, $(VO)HPO_4 0.5H_2O$.

2. Thermal decomposition of the hemihydrate vanadyl orthophosphate, with partial or total loss of the hydration water, formation of new phases.
3. Activation or aging inside the reactor; phase and morphological transformations, recrystallization.

3.1. Preparation of the precursor

Two main methods of preparation of the precursor can be singled out:

1. Reduction of V^{5+} compounds (V_2O_5) to V^{4+} in water by either HCl or hydrazine, followed by addition of phosphoric acid and separation of the solid by either evaporation of water or by crystallization.
2. Reduction of V^{5+} compounds in a substantially anhydrous medium with either an inorganic or an organic reducing agent, addition of dry phosphoric acid and separation of the solid obtained either by filtration, by solvent evaporation or by centrifugation.

A substantially anhydrous medium means the use of a dry organic solvent, of dry metal salts and components, as well as the use of phosphoric acid containing more than 98% H_3PO_4; moreover, the water formed by vanadium reduction and by digestion is removed by azeotropic distillation during the preparation.

There is general consensus that the necessary conditions to obtain an optimum catalyst are the following:

- synthesis in organic solvent of microcrystalline $(VO)HPO_4{\cdot}0.5H_2O$ with a preferential exposure of the (0 0 1) crystallographic plane;
- presence of stacking defects in the platelets;
- slight excess of phosphorus with respect to the stoichiometric amount; for instance, an atomic P/V ratio of 1.1 (the excess phosphorus remains strongly bound with the vanadyl acid phosphate).

Preparation in an anhydrous solvent is considered the best one to obtain active and selective catalysts. In all preparations essentially a single phase has been obtained, $(VO)HPO_4 0.5H_2O$. Only when a considerable excess of phosphorus ($P/V \gg 2$) is used, another phase may appear, $VO(H_2PO_4)_2$ [12]. When reduction of the V^{5+} compound is not complete, small amounts of V_2O_5 or $VOPO_4$ are also present which affect the nature of the products obtained by calcination [13].

The main differences observed between the several precursors regard the morphology of the $(VO)HPO_4 0.5H_2O$ crystallites obtained.

Fig. 2 shows the X-ray diffraction (XRD) patterns of the precursors prepared in organic and in aqueous media. The spectra confirm the results formerly published that the precursors prepared in an aqueous medium are more crystalline and exposure of the crystallographic plane (0 0 1) is less pronounced, since no preferential line broadening of the corresponding reflection is observed [11,12].

The following steps for the formation of the precursor in organic media (Scheme 1) can be proposed:

- formation of colloidal V_2O_5 at the water–alcohol interface; this has been proposed by O'Connor et al. [13], but according to Okuhara and Misono [14] it is not an important step;
- solubilization of V^{5+} through the formation of vanadium alcoholates [14] or of $VOCl_3$ in the case HCl is used as a reductant;
- reduction of the alcoholate in the liquid phase to solid V_2O_4 by the organic compound (the solvent itself or another more reactive alcohol such as benzyl alcohol) or by an inorganic reducing agent, such as HCl;
- reaction at the surface of V_2O_4 with H_3PO_4 to form $(VO)HPO_4{\cdot}0.5H_2O$ at the solid–liquid interface;
- separation of the precursor by filtration, centrifugation, decantation, and evaporation or by extraction of the solvent with a more volatile solvent followed by distillation under vacuum; alternatively, the precursor is washed with water to allow an organic layer to separate from an aqueous layer, followed by recovery of the precursor by drying.

The type of aliphatic alcohol used modifies the temperature at which vanadium is reduced; the reduction is kinetically controlled and complete only when benzyl alcohol is present (forming benzaldehyde and benzoic acid), when a long reduction time is used and after the addition of phosphoric acid [14]. It has also been observed that the type of alcohol may affect the morphology of $(VO)HPO_4 0.5H_2O$ [12].

In dry milling of the precursor, the rosette-like crystallites (formed when the preparation is carried

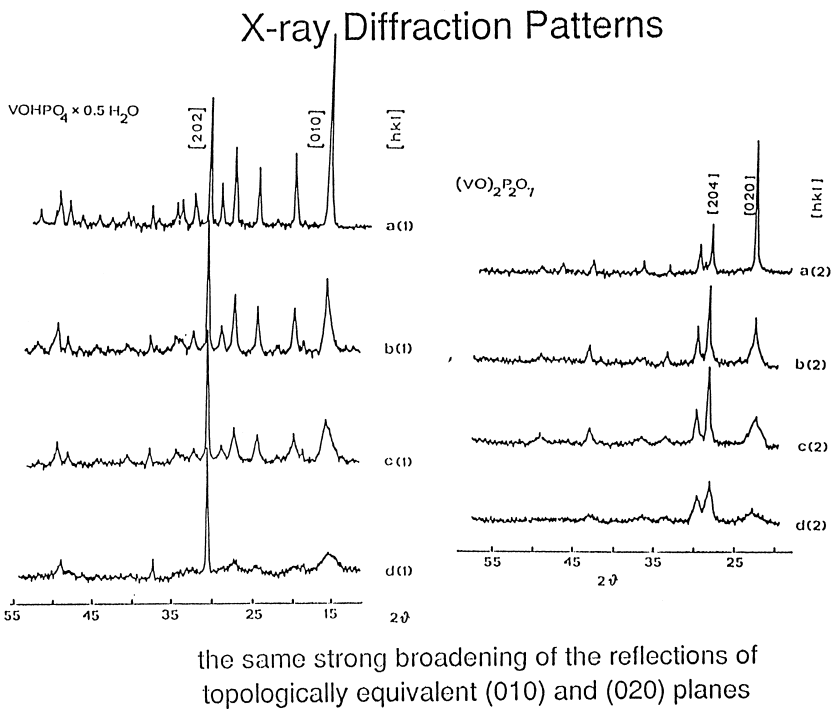

Fig. 2. X-Ray diffraction patterns of the precursor and the relative calcined phase of catalysts prepared in aqueous medium (a(1) and a(2)) and of catalysts prepared in organic medium (b(1), c(1), d(1) and b(2), c(2), d(2)). The number 1 is for the precursor, number 2 for the calcined catalyst.

out in isobutanol) can be broken and the effect is to decrease the (0 0 1) crystallographic plane exposure, while in wet milling shear forces allow the platelets to slide away, thus increasing the (0 0 1) exposure [12].

In the preparation in the presence of benzyl alcohol many authors report the formation of platelets with stacking faults (deduced from the preferential line broadening of the (0 0 1) reflection) attributed to the trapping of the alcohol between the layers of the precursor and its release during activation [11,12,14].

In the preparation in an aqueous medium the following steps for the formation of the precursor can be proposed:

- reduction of V_2O_5 to soluble V^{4+};
- after addition of H_3PO_4 no precipitation occurs, due to the strong acid conditions [11];
- development of $(VO)HPO_4 0.5H_2O$ with another spurious amorphous phase only after complete evaporation of the solvent [15];
- alternatively, crystallization of pure $(VO)HPO_4 0.5H_2O$ by addition of water when the solution is highly concentrated (when it is very viscous) [11], or by seeding under hydrothermal conditions (high temperature and steam pressure).

3.2. Thermal dehydration of the precursor

Thermal dehydration of the precursor is usually realized with a multistage procedure. The first stage is roasting at temperatures lower than 300°C in order to eliminate the organic impurities or chlorine ions from the precursor without however causing dehydration to occur.

After this treatment, different types of thermal dehydration have been proposed:

1. Dehydration inside the reactor starting from a low temperature (280°C) in a flow of a lean reactant mixture and at low flow rate until standard operating conditions are reached in approximately one day.
2. Dehydration in an oxygen-free atmosphere at temperatures higher than 400°C, followed by

introduction of the reactant mixture (*n*-butane in air). With this procedure, after the first step, crystalline $(VO)_2P_2O_7$ is obtained, which after the introduction of the reactant mixture can remain substantially unmodified or be partially or totally reoxidized to a V^{5+}-containing phase [12,15–17].

3. Single or multistep calcination in air until a temperature lower than 400°C is reached, and then introduction of the reactant mixture [12,15,16].

Controversial results are found in the literature, regarding especially the transformation of precursors to the active phase, because many different phases can form depending on:

- temperature, time and atmosphere of treatment;
- morphology of the precursor;
- P/V ratio;
- presence of additives; and
- presence of defects in the structure.

After calcination at 280°C, the precursor is still present during release of the trapped benzyl alcohol, and this release leads to disruption of the structure [15], causing an increase in the surface area.

Fig. 3 shows the evolution of the XRD patterns of the precursor prepared in an organic medium when it is treated in air at high temperature. When the precursor is maintained at 380°C in air, the reflections typical of vanadyl orthophosphate progressively decrease in intensity, while evident amorphization occurs [15]. When the diffraction lines of the precursor have disappeared completely, only an amorphous material remains. After 3–6 h at 380°C in air, the sample is highly amorphous, and weak reflections relative to the vanadyl pyrophosphate and to a V^{5+} phase are observed. Transformation to the well-crystallized $(VO)_2P_2O_7$ occurs in the reactor, after several hundreds of hours of time-on-stream.

Different types of $VOPO_4$, more or less reducible to $(VO)_2P_2O_7$, have been identified. Key factors in catalyst preparation to avoid the oxidation of $(VO)_2P_2O_7$ and/or of the intermediate amorphous phase to a V^{5+} phosphate, the formation of which is known to be deleterious for activity and selectivity [18,19], are the following:

- *The* P/V *ratio*. P/V ratios in the precursor higher than the stoichiometric one stabilize the $(VO)_2P_2O_7$ not only in the reactant atmosphere but also for calcination in air at high temperature.
- *Minimization of impurities*. The presence of free V_2O_5 [13], even in traces, or of additives such as Mn^{2+} [7] facilitates the oxidation of the pyrophosphate in the reactant atmosphere.
- *Morphology*. It has been proposed that oxidation of $(VO)_2P_2O_7$ starts at the side faces of the (1 0 0) plane [7]. Catalysts with a higher exposure of this

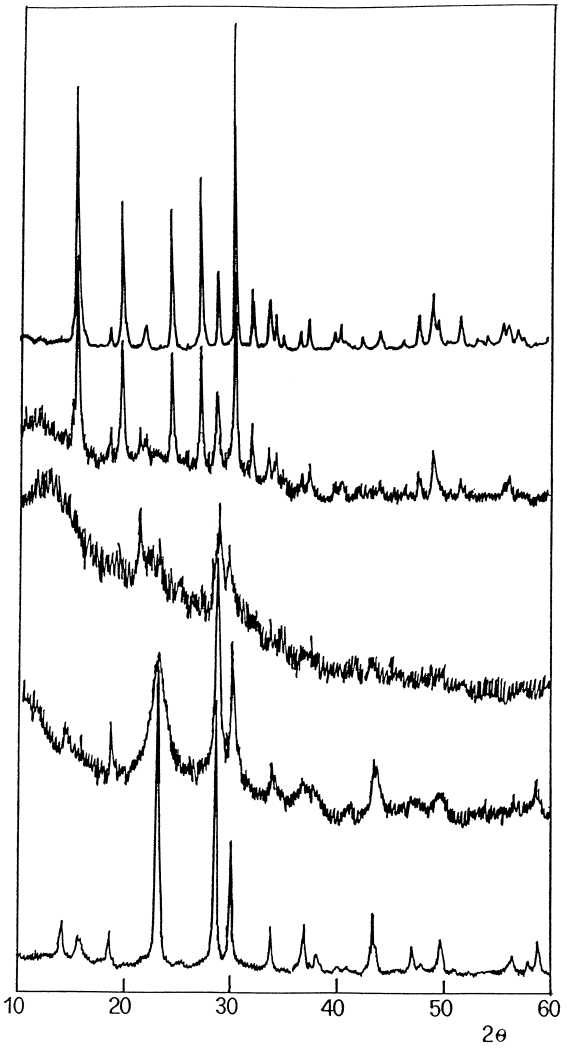

Fig. 3. Ex situ evolution of $(VO)HPO_4 0.5H_2O$ at 380°C in air. Top: precursor; intermediates: samples at increasing calcination time; bottom: equilibrated catalyst $(VO)_2P_2O_7$.

plane, such as those prepared in an organic medium, are therefore less oxidized.

- *Low temperature treatment in oxygen-containing atmosphere*. Precursors prepared in an organic medium and which contain defects transform at lower temperatures than those prepared in an aqueous medium that are more crystalline.
- *Additives*. The presence of Zn^{2+} as a promoter avoids overoxidation of the catalyst at high temperature [14].

By means of electron microscopy [12,14] it has been observed that the dehydrated phases maintain the morphology of the precursor. Moreover, XRD analysis has shown that broadening of reflections relative to the basal plane of the precursor also occurs for the reflections relative to (*h* 0 0) crystallographic planes (parallel to the basal plane) of $(VO)_2P_2O_7$; the reflection relative to the (2 0 0) plane looks particularly broadened.

These findings, together with analogies of the two structures, allowed Bordes [18] to propose that the transformation from $(VO)HPO_4 0.5H_2O$ to $(VO)_2P_2O_7$ is topotactic.

It has been found [20] that different phases present in calcined catalysts can cooperate to improve the catalytic behaviour. These findings are very likely to be less important for the most active and selective catalysts, where only one phase has been detected, but they can be important in the stage of formation and as regards the catalytic properties of vanadyl pyrophosphate during the activation procedure.

Scheme 1 summarizes the possible evolution of $(VO)HPO_4 0.5H_2O$ with temperature.

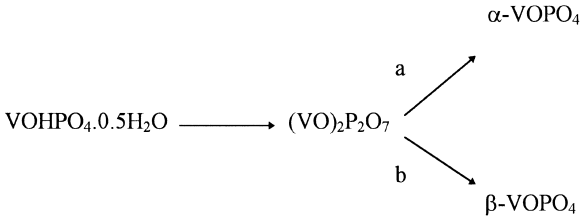

a) Strong conditions

b) Mild conditions

Scheme 1.

3.3. Activation/aging procedure

After the stage of dehydration the catalyst has to be activated; this stage can be carried out either in the presence of or without an *n*-butane/air atmosphere. During prolonged exposure to the reactant atmosphere changes occur with time-on-stream both in catalytic behaviour and in the physico-chemical properties of the catalyst.

In catalysts calcined in air the transformation from a partially amorphous, possibly oxidized compound to an almost completely crystalline vanadyl pyrophosphate inside the reactor and in the presence of the reactant mixture requires more than 100 h, depending on the features of the fresh catalyst, i.e. the calcination conditions employed.

If the fresh catalyst is highly oxidized (sample A in Fig. 4), after 80 h time-on-stream the $(VO)_2P_2O_7$ has in part crystallized, but the catalyst is yet oxidized. More than 500 h are necessary to reduce V^{5+} completely and obtain well-crystallized vanadyl pyrophosphate. When the fresh catalyst is only slightly oxidized (i.e., after a milder calcination treatment, sample B), a period of 80 h time-on-stream leads to an increase in crystallinity. In this case the final crystalline compound is obtained in a shorter period of time (200–300 h), because vanadium is already in the reduced state. Fresh catalyst has been designated as non-equilibrated and a catalyst after prolonged time-on-stream as equilibrated.

A more precise definition of an ''equilibrated'' catalyst has been recently given by Ebner and Thompson [21]. According to these authors, an ''equilibrated'' catalyst is one which has been kept in a flow of *n*-butane with a concentration of 1.4–2% in air and at least GHSV 1000 h^{-1}, for approximately 200–1000 h.

The features of the ''equilibrated'' catalyst are the following [21]:

- Average degree of oxidation of vanadium, 4.00–4.04.
- Bulk P/V ratio, 1.000–1.025.
- XPS surface atomic P/V ratio, 1.5–3.0.
- BET surface area, 16–25 $m^2 g^{-1}$.

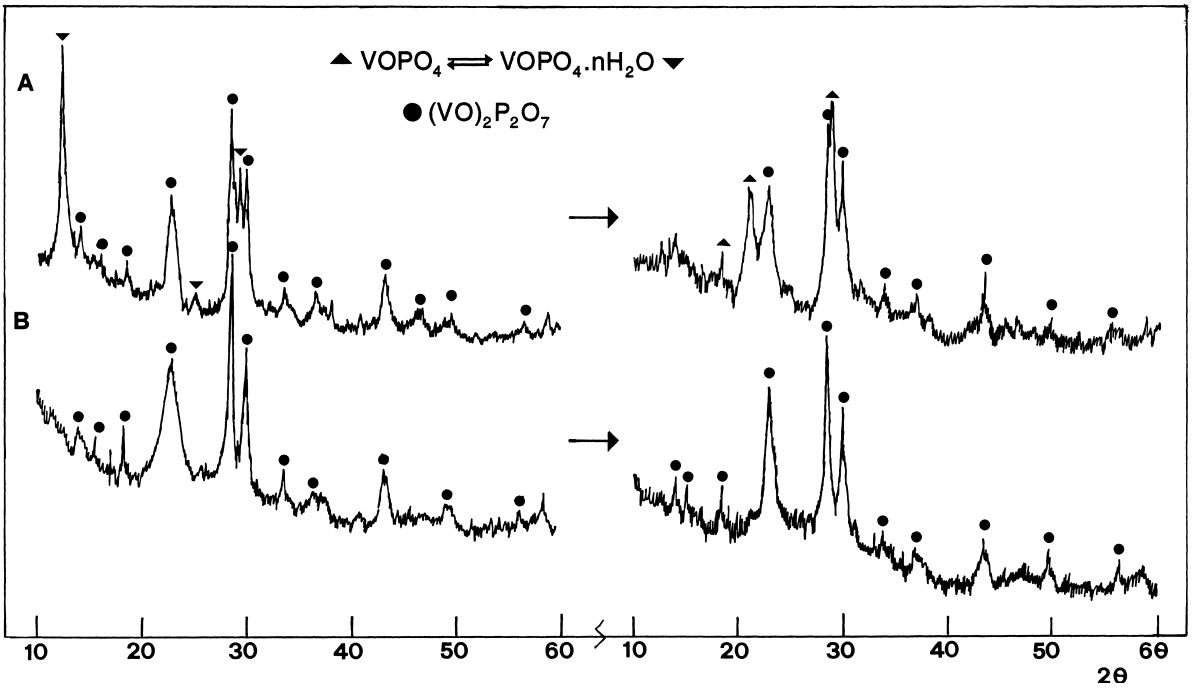

Fig. 4. XRD patterns illustrating the structural evolution of fresh catalyst in the reaction environment. Samples were obtained by static calcination in air at 380°C for 30 h (A) and 2 h (B). The precursor contained 5% of organic binder.

- X-ray diffraction pattern, vanadyl pyrophosphate.
- Morphology, rectangular platelets and rod-like structures.

4. The chemistry of preparation of V/Ti/O mixed oxides

V/Ti/O are the catalysts for the oxidation of *o*-xylene to phthalic anhydride. Different methods of preparation have been proposed:

1. Grafting of $VOCL_3$ with hydroxylated TiO_2 surface in an organic solvent.
2. Wet impregnation of TiO_2 from a solution of soluble vanadium species in water.
3. Coprecipitation of vanadium and titanium species.
4. Solid state reaction between V_2O_5 and TiO_2.

We shall discuss here only the method of preparation by solid state reaction.

4.1. Preparation by solid state reaction

The preparation by solid state reaction has been obtained through the following three steps:

1. gentle mixing of the oxides;
2. calcination in air at 500°C for 24 h; and
3. activation inside the reactor with the presence of the reagents at different temperature and residence time and *o*-xylene concentration until the values used in standard conditions in the industrial plant are reached [3,22–25].

4.1.1. Formation of an interacting V^{IV} layer

The solid state reaction of the V_2O_5 and TiO_2 in air at temperatures in 400–500°C ranges, leads, in the absence of any reducing agent, to the formation of relevant amounts of V^{IV}. The method used to characterize the catalyst by chemical analysis is reported in Table 5.

Table 5
Characterization of V–Ti mixed oxide by chemical analysis

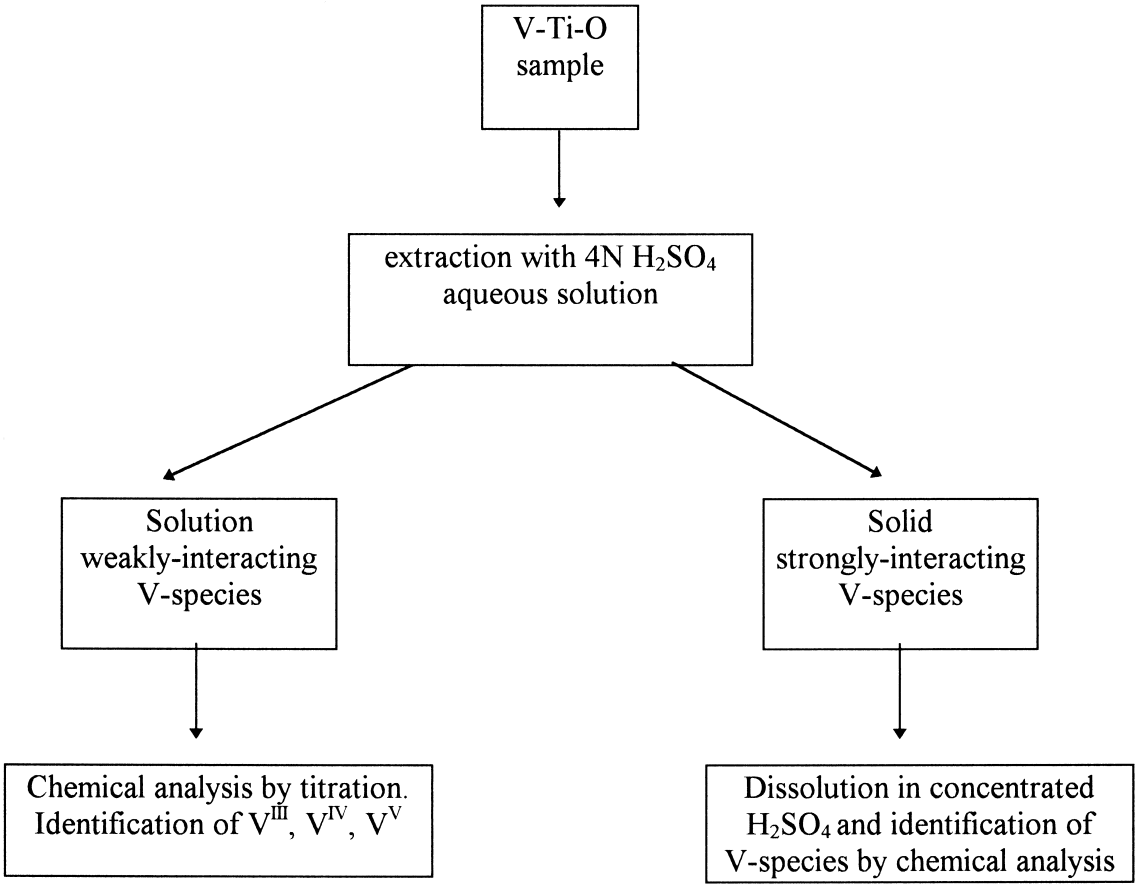

Chemical analysis shows the formation of V^{IV} species that cannot be desolved in acid or basic aqueous medium in contrast to other supported V^{IV-} and V^{V} oxides species. The amounts of V^{IV} formed during the calcination of V_2O_5 and TiO_2 that is approximately equal (for catalysts with a surface area of about 10 $m^2\ g^{-1}$) to the reference monolayer estimated on the basis of a geometrical coverage of the titania surface are reported in Table 6. The reference monolayer is about 0.1% w/w of V_2O_5 per m^2 of TiO_2. For the sake of comparison the amounts of the various species of vanadium determined by chemical analysis are all expressed in Table 6 as % by weight of equivalent mole of V_2O_5 [24].

The formation of these V^{IV} surface sites probably occurs by specific reaction between hydroxyl group of TiO_2 surface and V^{V} sites and the formation of these species is the driving force for the spontaneous reduction of V^{V} in oxidizing conditions and for its surface migration. The mechanism of the formation probably involves the preliminary formation of Ti^{3+} sites by dehydroxylation with consecutive electron transfer to V sites and formation of stable Ti–O–V bond.

Table 6
Relative amounts of V-species formed on anatase (s.a. 9.8 $m^2\ g^{-1}$) in sample prepared by solid state reaction through V_2O_5

Preparation step	Equivalent of V_2O_5 vs. TiO_2 (w/w%)			
	V^{IV} (insoluble)	V^{V} (insoluble)	V^{IV} (soluble)	V^{V} (soluble)
(a)	—	—	—	7.7
(b)	0.9	—	—	6.8
(c)	0.9	—	6.8	—
(d)	0.9	—	0.3	6.5
(e)	0.9	—	3.1	3.7
(f)	0.9	—	2.0	4.8

Note: (a) mixing; (b) calcination at 500°C for 24 h in air; (c) activation in the presence of a reducing agent (10% v/v of NH_3); (d) sample (c) after calcination at 400°C for 3 h; (e) sample (a) after heating at 320°C in flow of *o*-xylene/air for 24 h or (f) for 1440 h.

In contrast to what happens with rutile samples, the addition of a reducing agent during the heat treatment does not further increase the amount of insoluble V^{IV} in anatase sample (Table 6).

Similar results are obtained if the heat treatment is performed in situ during the catalytic tests (Table 6). In rutile samples, the amount of insoluble V^{IV} increases further up to a limiting value of around 3.8% w/w after long-term catalytic tests. The redox and chemical (solubility) properties of the V^{IV} sites are altered considerably by the interaction with the TiO_2 surface, in comparison with those of the V^{IV}-oxide. XRD and EPR data clearly exclude the formation of a solid solution in anatase samples, in contrast to that observed for rutile samples. In particular, ESR characterization [25] shows the presence in anatase samples of several isolated surface and unsaturated vanadyl ions in slightly different distorted octahedral environments. Some of these species may interconvert with each other by the addition of suitable probe molecules, indicating the presence of Lewis acid. In rutile samples, in contrast, no isolated surface vanadyl species could be detected, even for amounts of insoluble V^{IV} species much below those necessary for monolayer coverage. The ESR spectrum is always characterized by a broad unstructured signal with a *g* value of about 1.98 that is characteristic of near-lying V^{IV} paramagnetic centres. This broad signal is overlapped by another signal showing hyperfine structure which can be attributed to isolated non-vanadylic V^{4+} sites in substitutional positions in the rutile structure.

Table 7
Fraction of insoluble V^{IV} in anatase and in rutile, reduced (in 2% H_2 in He) and reoxidized (with 20% O_2 in N_2) at 400°C

Sample	Insoluble V^{IV} (w/w%)	V^{IV} (atoms%) after reduction	V^{IV} (atoms%) after reoxidation
Anatase	0.9	100	0
Rutile	3.7	24	23

A further difference characterizes the insoluble V^{IV} sites in anatase and rutile samples (Table 7). In anatase sample all the V^{IV} sites could be reduced and are accessible to gaseous reactants such as H_2, while only a fraction (20–30%) of the soluble V^{IV} sites in rutile samples are accessible to gaseous reactants, indicating that only a reduced fractions of these sites is localized at the surface or in subsurface layers. A further difference between insoluble V^{IV} sites in anatase and rutile samples is shown in Table 7. V^{IV} sites can be more easily reduced to V^{III} in anatase samples as compared to rutile samples, but cannot be oxidized to V^{V} as occurs in rutile samples.

ESR and reactivity data thus indicate a homogeneous distribution of these V^{IV} sites on the surface of anatase, with a mean estimated distance of 4.5 Å from V centres and the presence of islands of V_2O_4 on the surface of the rutile sample.

The presence of these V^{IV} surface sites also modifies the reactivity in *o*-xylene oxidation of titania which is enhanced considerably as compared to pure TiO_2, even though the activation of *o*-xylene is relatively not selective to phthalic anhydride improves with time-on-stream in the rutile sample as the consequence of the possibility of oxidation of insoluble V^{IV} to V^{V} in these catalyst (see Table 7).

4.1.2. Nature of the active layer

On the V^{IV} modified surface of TiO_2 after calcination only V_2O_5 crystallites are present, but this phase transforms to a partially reduced amorphous phase during the consecutive in situ treatment in a flow of *o*-xylene/air (Table 7). Stable catalytic behaviour may be reached in 500 h of time-on-stream. The characterization of the nature of the upper layer on V^{IV}-modified TiO_2 surfaces may be realized after this extraction with a dilute sulphuric acid solution. The analysis of this upper layer indicated: (i) a mean valence state of vanadium of 4.71 that corresponds

to a V^V:V^I ratio of 2:1 and (ii) the presence of a characteristic IR band centred at 995 cm^{-1} due the symmetrical stretching mode of V^V=O.

The removal of this phase decreases the activity in *o*-xylene oxidation but especially the selectivity, which drops from 75% to 30%. The phase is XRD amorphous and no evidence was found of the presence of residual V_2O_5 crystallites characterized by a defined sharp band at 1020 cm^{-1} of V=O stretching mode. The shift to lower frequencies of V^V=O in comparison to crystalline V_2O_5 may be attributed to an electronic effect of neighbouring V^{IV} sites or to the presence of coordinatively adsorbed water that causes a weakening of the V^V=O double bond. In general, FT-IR spectra of the catalyst after different times show that a good correlation exists between the frequency of the V=O stretching band in the samples and the oxidation states of the vanadium oxides deposed on the surface of the TiO_2. The band changes position in the spectrum and decreases in frequency from 1020 cm^{-1}, corresponding to pure crystalline V_2O_5, to lower values proportional to the degree of the reduction. In agreement the consecutive oxidation of a V–TiO_2 sample after long running catalytic tests indicates a shift to higher frequencies and the appearance of a further band at about 1010 cm^{-1}. A corresponding increase in the mean oxidation state of vanadium from 4.72 to 4.91 is observed. This suggested that the modification of initial V_2O_5 particles in the reaction medium is not completely reversible by consecutive reoxidation.

Similar results are found in rutile samples, but both the time necessary to reach a certain mean valence state of vanadium as well as the stability of the reduced catalyst against consecutive oxidation are indicative of the formation of less stable, partially reduced, vanadium-oxide species on the rutile surface in comparison to the anatase surface.

Wide line solid state ^{51}V-NMR characterization of the local coordination of V^{5+} sites in the active phase [24] indicates a significant shift of the asymmetric resonance peak due to axial shielding and a general broadening of the peak as compared to the reference signal for V_2O_5. The change is analogous to that observed in hydrated V_2O_5 and could be interpreted as a change from the nearly five-fold coordination of vanadium in the initial crystalline V_2O_5 to a nearly octahedral coordination in the active phase after long-term catalytic tests. No great differences in the ^{51}V-NMR spectra are observed in the anatase and rutile samples after long-term catalytic tests.

XPS characterization of the depth profile of vanadium in anatase samples [24] shows a considerable change in the V/Ti atomic ratio (from about 0.47 to 0.27) after removal of the first nm of thickness from the catalyst using Ne^+ ions for the sputtering. The V/Ti atomic ratio then decreases at a slower rate to nearly zero with the removal of a further 12–14 nm. In rutile samples, on the contrary, the presence of the first monolayer species is not observed, but rather only the second species.

4.1.3. Dynamics of in situ evolution

Fig. 5 shows that the V_2O_5–TiO_2 catalyst in a pilot plant reactor undergoes a first deep reduction and then partial reoxidation with the formation of the final active catalyst whose characteristics were discussed above.

The V_2O_5 is first reduced to a phase with a valence state similar to that of V_6O_{13}, however XRD analysis shows the presence of only an amorphous vanadium-oxide phase. It is thus not possible to make a definite attribution. After this stage, the catalyst starts to be progressively reoxidized and reaches a final stable mean valence state in the soluble part of vanadium similar to that present in the V_3O_7 phase. Also in this case, the vanadium-oxide phase is XRD amorphous. It should be noted that the crystalline V_3O_7 is prepared by solid state reaction of V_6O_{13} with V_2O_5 [25] and it is reasonable to hypothesize that a similar mechanism occurs in the transformation of the V_2O_5–TiO_2 mixture to the final active catalyst. The correlation of this effect with a catalytic behaviour is complex because two different catalytic effects take place at the same time: (1) the spreading of vanadium on the TiO_2 surface, and (2) the reduction and consecutive partial oxidation of the V-oxide upper layer and the consequent change in the nature of the supported phases.

In order to obtain a better understanding of the dynamics of these redox transformations as well as the role of titanium oxide in determining the final state of the catalyst, we carried out an analogous experiment where the evolution of an unsupported pure commercial V_2O_5 (Fig. 6) was followed. In this case, the concurrent process of spreading of vanadium-oxide on the surface of the titanium oxide is not present.

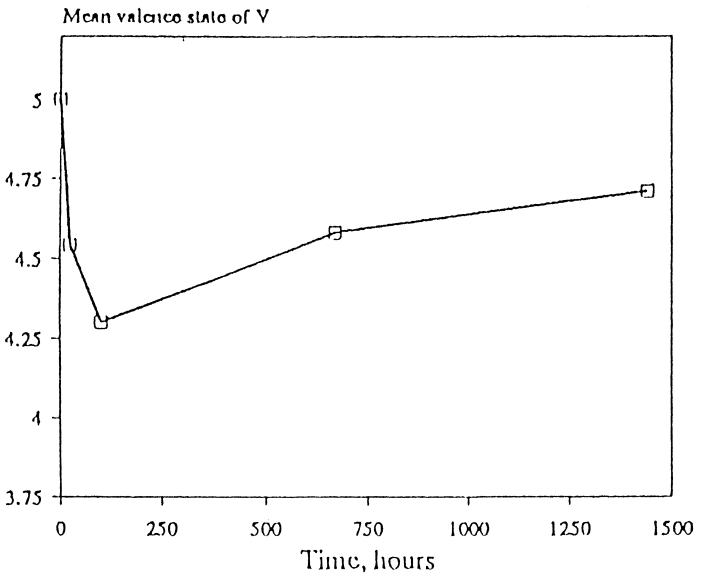

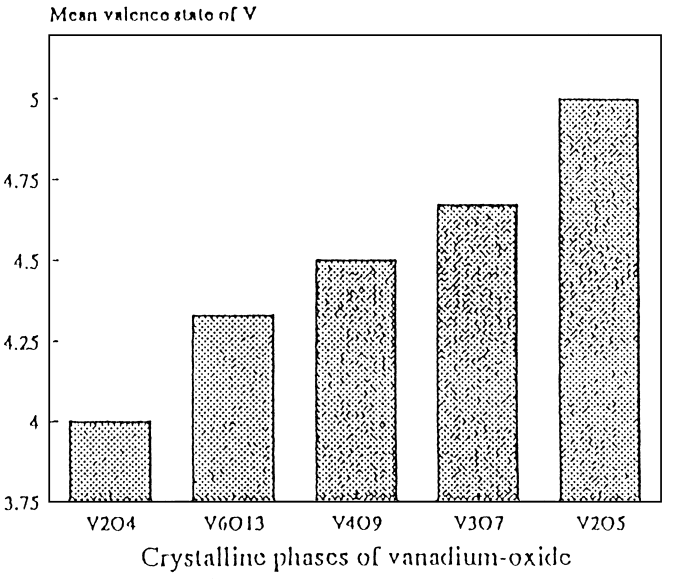

* Formation of a V-oxide phase with $V^{V}:V^{IV} = 2:1$ corresponding to V_3O_7
* The active phase forms through a first deep reduction with consecutive reoxidation to a V3O7-like phase.

Fig. 5. Change of valence state of V (soluble part) as a function of time on stream during *o*-xylene oxidation.

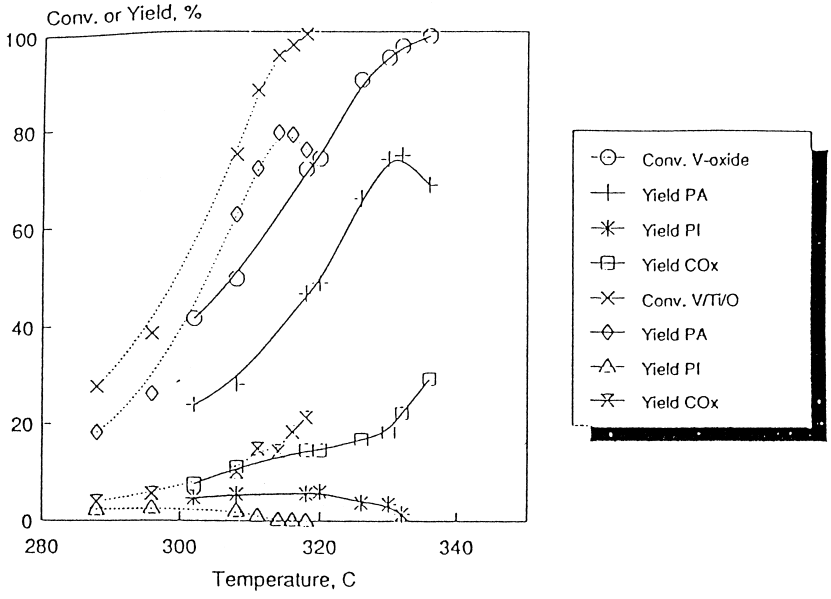

Fig. 6. Effect of reaction temperature on the catalytic behaviour of VTiO samples (dashed line) and of pre-reduced unsupported V-oxide (solid line).

The commercial V_2O_5 also undergoes a similar reduction–reoxidation process of the supported V_2O_5 (Fig. 6), but the parallel change in the catalytic behaviour may be more clearly correlated to the dynamics of phase transformation. The selectivity in phthalic anhydride is very high at the beginning, but decreases reaching a minimum value after about 40 h, and then increases by further in situ treatment up to about 200 h.

A parallel evolution is observed in the activity, whereas the selectivity to CO_x and phthalide pass through a maximum. In the IR spectrum of V_2O_5 after in situ conditioning is very different from that shown by V_2O_5 supported on TiO_2 after similar treatment (a broad band centred at around 995 cm^{-1}) even though in the latter case frequencies below about 900 cm^{-1} cannot be analysed due to a strong adsorption of TiO_2 band. The differences in the bands in the 900–1100 cm^{-1} region may suggest that the nature of the final vanadium-oxide active phase on TiO_2 is different from that found for the unsupported V_2O_5, notwithstanding the analogous V^V:V^{IV} ratio of 2:1 and the relatively similar catalytic behaviour. The selectivity to phthalic anhydride on the V-oxide supported on TiO_2, in fact, is about 75%, at 95% conversion compared to a selectivity of about 68% of unsupported V_2O_5. The lowering of the selectivity to phthalic anhydride in the latter case is mainly due to the formation of a large amount of phthalide rather than to the formation of a larger amounts of CO_x.

In order to verify further the relationship between in situ evolution of the catalyst and the catalytic behaviour, the time-on-stream evolution of a pre-reduced vanadium oxide catalyst was followed. This catalyst was prepared by precipitation of V^{IV} and calcination for a short time at 280°C. The mean valence of the starting sample was 4.84, near to that found at the end of the evolution of the V_2O_5-based catalyst.

This sample, after an initial rapid in situ modification, shows an almost constant catalytic behaviour over a long time. It exhibits good activity and good selectivity in phthalic anhydride (Fig. 7) comparable to that of pure V_3O_7 and the final valence state after the catalytic test is 4.62. These data further indicate that, notwithstanding the differences in the V-oxide phases present in supported or unsupported V_2O_5-based catalyst, the same selectivity and maximum yield to phthalic anhydride can be observed when a suitable starting V-oxide is used.

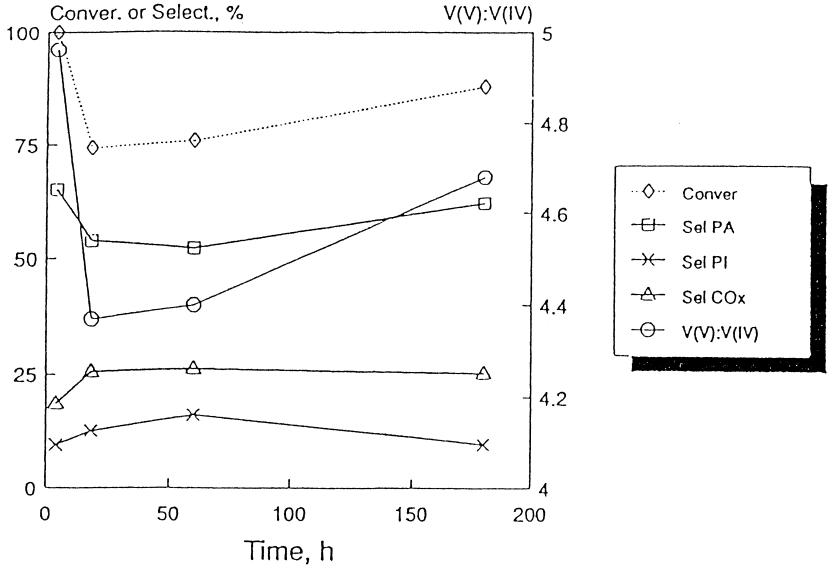

Fig. 7. Effect of time on stream on the catalytic behaviour in *o*-xylene conversion at 327°C and on the mean valence state of vanadium of a commercial V_2O_5 sample.

References

[1] F. Trifirò, P. Forzatti, P.L. Villa, Preparation of Catalyst, Elsevier, Amsterdam, 1996.
[2] F. Cavani, F. Trifirò, Preparation of Catalyst, Elsevier, Amsterdam, 1995.
[3] G. Centi, M.L. Granados, D. Pinelli, F. Trifirò, Structure–Activity Relationship in Heterogeneous Catalysis, Elsevier, Amsterdam, 1991.
[4] H. Voge, C.R. Adams, Adv. Catal. 17 (1967) 151.
[5] F. Trifirò, C. Banfi, G. Caputo, P. Forzatti, I. Pasquon, J. Catal. 30 (1973) 393.
[6] F. Trifirò, C. Banfi, G. Caputo, P.L. Villa, J. Less Common Metals 36 (1974) 305.
[7] F. Trifirò, H. Hoser, R.D. Scarle, J. Catal. 25 (1972) 12.
[8] P.L. Villa, G. Caputo, F. Scala, F. Trifirò, J. Catal. 25 (1972) 12.
[9] M.J. Schwing-Weill, Bull. Soc. Chim. France (1972) 2515.
[10] Patent N.25545 A 74 Ital. Appl. 25.7.74.
[11] F. Cavani, F. Trifirò, Appl. Catal. A 88 (1992) 115.
[12] H.S. Horowitz, C.M. Blackstone, A.W. Sleight, G. Teufer, Appl. Catal. 38 (1988) 193.
[13] M. O'Connor, F. Dason, B.K. Hodnett, Appl. Catal. 64 (1990) 16; 12 (1988) 91.
[14] T. Okuhara, M. Misono, Catal. Today 16 (1993) 61.
[15] L.M. Cornaglia, C. Caspani, E.A. Lombardo, Appl. Catal. 74 (1991) 15.
[16] R.M. Contractor, J.R. Ebner, M.J. Mummey, in: G. Centi, F. Trifirò (Eds.), New Developments in Selective Oxidations, Elsevier, Amsterdam, 1990, p. 553.
[17] I. Matsuura, M. Yamazaki, in: G. Centi, F. Trifirò (Eds.), New Developments in Selective Oxidation, Elsevier, Amsterdam, 1990, p. 563.
[18] E. Bordes, in: R.K. Grasselli, A.W. Sleight (Eds.), Structure–Activity and Selectivity Relationships in Heterogeneous Catalysis, Elsevier, Amsterdam, 1991, p. 21.
[19] F.B. Abdelouahab, R. Olier, N. Guilhaume, F. Lefebvre, J.C. Volta, J. Catal. 134 (1992) 151.
[20] P. Ruiz, Ph. Bastians, L. Caussin, R. Reuse, L. Daza, D. Acosta, B. Delmon, Catal. Today 16 (1993) 99.
[21] J.R. Ebner, M.R. Thompson, Catal. Today 16 (1993) 51.
[22] F. Cavani, E. Foresti, F. Parrinello, F. Trifirò, Appl. Catal. 38 (1988) 311.
[23] F. Cavani, G. Centi, F. Parrinello, F. Trifirò, in: B. Delmon, P. Grange, P. Jacobs, G. Poncelet (Eds.), Preparation of Catalyst IV, Elsevier, Amsterdam, 1987, p. 227.
[24] G. Centi, E. Giamello, D. Pinelli, F. Trifirò, J. Catal. 130 (1992) 220.
[25] G. Centi, D. Pinelli, F. Trifirò, D. Ghoussoub, M. Guelton, D.L. Gengembre, J. Catal 130 (1991) 238.